In Situ Determination of Variation of Poisson's Ratio in Granite Accompanied by Weathering Effect and its Significance in Engineering Projects

AUTHOR(S):

KITSUNEZAKI, Choro

CITATION:

KITSUNEZAKI, Choro. In Situ Determination of Variation of Poisson's Ratio in Granite Accompanied by Weathering Effect and its Significance in Engineering Projects. Bulletin of the Disaster Prevention Research Institute 1965, 15(2): 19-41

ISSUE DATE:

1965-11-30

URL:

http://hdl.handle.net/2433/124701

Bulletin of the Disaster Prevention Research Institute Vol. 15, Part 2, No. 92, Nov., 1965

In Situ Determination of Variation of Poisson's Ratio in Granite Accompanied by Weathering Effect and its Significance in Engineering Projects

By Chōrō KITSUNEZAKI

(Manuscript received September 30, 1965)

Abstract

At first, the practical method for the generation of S wave was examined in the adit. A small explosion in a drill hole was mainly used as its wave source. The small explosion can be approximately considered as the single force referring to the effect on the generation of S wave.

Secondly, real measurements were carried out in order to determine the ratio (α) of P wave velocity (V_p) to S wave velocity (V_s) in granite. It was approximately expressed by the following formula.

$$\alpha = -0.49V_p + 4.34$$

where V_p [km/sec] is the value which varies by the weathering effect. It is suggested by this result that the well-known discrepancy between dynamic Young's modulus and static Young's modulus, in situ, can be explained by neglecting Poisson's ratio variation in the estimation of dynamic Young's modulus, and partly by insufficient evaluation of the velocity lowering in the adit wall.

§ Introduction

Determination of elastic constants of rocks is ofen required for designs in civil engineering. Seismic prospecting is applied to measure elastic constants of rocks in situ. The most important advantage of this method is that physical properties of rocks in a wide and deep range can be measured in its natural conditions. However, it is generally recognized that Young's modulus determined by this method is different from one determined by the direct mechanical method, the jack method.[1)~3)] For convenience we shall call the former the dynamic method and the latter the static method. The values found by the dynamic method are larger than those by the static method. According to several reports[1)2)], the ratios of these were about four to five. Many ideas were proposed to explain this problem. However, little attension has been paid to the physical basis for the determination of Young's modulus, that is, the assumption on Poisson's ratio.

Properties of isotropic and elastic materials can be represented only by two constants. Two elastic constants can not be determined by one value. So, an assumptive value has been used as Poisson's ratio for the estimation of Young's modulus, because the kind of the seismic waves whose velocity can

be practically measured has been considered as only P wave. Here is one problem in the validity of the assumption for Poisson's ratio. Between P wave velocity V_p, S wave velocity V_s, Poisson's ratio σ, density ρ, and Young's modulus E, is the following relation,[5]

$$E=\rho V_p^2 f(\sigma) \tag{1}$$

where

$$f(\sigma)=\frac{(1+\sigma)(1-2\sigma)}{(1-\sigma)} \tag{2}$$

$$\sigma=\frac{\alpha^2-2}{2(\alpha^2-1)} \tag{3}$$

If we take V_p/V_s in place of σ,

$$E=\rho V_p^2 F(\alpha)\times 10^{10}\text{dyne/cm}^2 \tag{4}$$

$$=1.02\rho V_p^2 F(\alpha)\times 10^4\text{kg/cm}^2 \qquad \text{(engineering unit)}$$

where

$$\alpha=V_p/V_s, \quad V_p=[\text{km/sec}] \quad \rho=[g/\text{cm}^3] \tag{5}$$

$$F(\alpha)=\frac{3\alpha^2-4}{\alpha^2(\alpha^2-1)}=f(\sigma) \tag{6}$$

The relations between α, σ and $F(\alpha)$ are shown in Fig. 1.

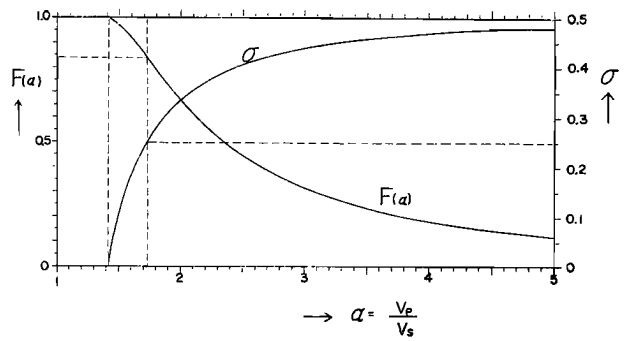

Fig. 1 Relation between Poisson's ratio σ, $F(\alpha)$ and α.

Existence range is 0 to 0.5 for σ, 1.414 to ∞ for V_p. In general cases,[1)-4)] Poisson's ratio σ is assumed as 0.25 ($V_p=1.73$), disregarding diverse states of rock. This figure is valid for the materials in the interior of the earth, and the laboratory experiments[6)] for rock specimens revealed an approximate validity of this figure. Usually, however, the laboratory experiments are carried out not for weathered rock specimens with cracks, but for sound rock specimens. Can the application of this figure be extended to the rocks in natural condition, based only on such laboratory experiments? If this assumption is not valid, considerable changes are possible for the estimated Young's modulus (Fig. 1). For this reason, the author intends to measure Poisson's ratio in situ. As known from Eq. (3), Poisson's ratio can be determined by the measurements of P wave velocity and S wave velocity.

§ Experimental field

Experimental data in this paper, unless otherwise specified, were obtained in the field experiment at the geological survey area for the construction of

a power plant in the Tsuruga Peninsula, Fukui Prefecture, Japan. The place is situated in a granitic zone. Geological survey classifies the rock of the experimental field to granite, granite-pophyry and aplite. But the detail of zoning may not be necessary at the present stage of discussion. In this paper they are simply looked as granite. The position of the field is marked on the map in Fig. 2, as well as a few other experimental fields cited in this paper. The rock is characterized by development of a regular joint system, dominantly striking N65°E and dipping 74°SE. Shear zones also tend to dominate along this plane. The experimental works were carried out in the exploration adit, about 20m below the mean sea level and about 25m–70m below the ground surface. The map of the adit is shown in Fig. 3. The classification of the feature of rock specified in the map is cited from H. Tanaka's survey (see, Appendix). Seismic velocites were measured in the rocks of variable state—sound to weathered.

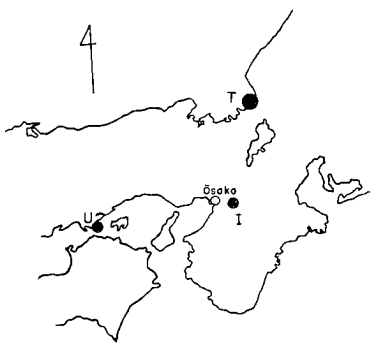

Fig. 2. The places of experimental field.
T: Tsuruga (main field).
I: Ikoma
U: Ushimado.

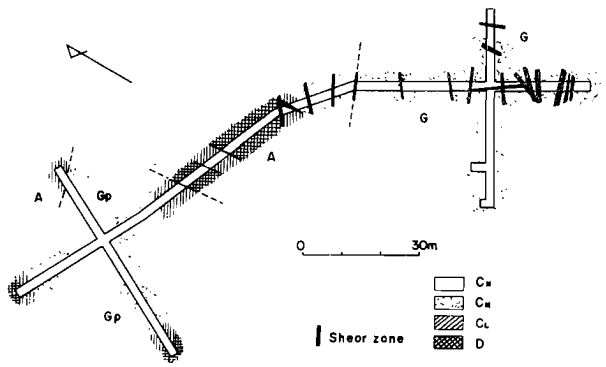

Fig. 3. Geological condition of the experimental field (adit).
G: granite. *Gp*: granite-porphyry.
A; aplite. --- boundary of rocks.

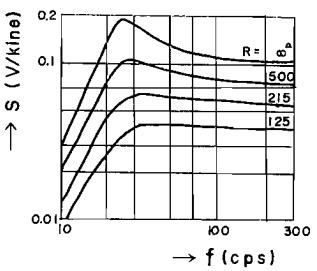

Fig. 4. Frequency characteristics of the geophone.

§ Experimental apparatus

A conventional recording system consisting of geophones, an amplifier and an electro-magnetic oscillograph was used in this experiment. However, each unit was selected considering the speciality of the work. The geophones, NEC VP-225, have natural frequency of 25cps and can be used for the detection of horizontal vibration as well as vertical vibration. The amplifier, ST-2600A, is a transistorized one (12 elements) manufactured by Tōkyō-Shibaura Electric Company at the special order of our laboratory. Its important characteristics are as follows. Amplifing range covers relatively high frequency one, 30—3000 cps, and multiple filter units of high and low cut are set. Consideration is paid to the accurate measurement of wave form and amplitude.

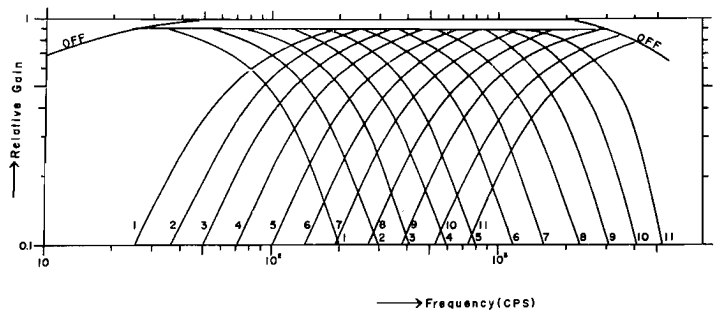

Fig. 5. Frequency characteristics of the amplifier.

Frequency characteristics of the geophone are shown in Fig. 4, that of the amplifier in Fig. 5.

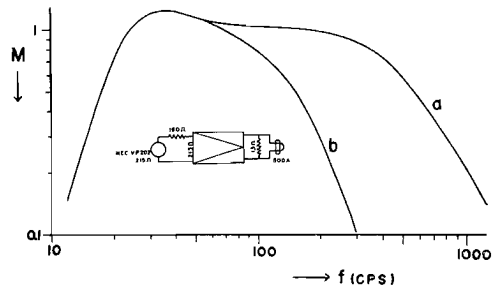

Fig. 6. Resultant frequency characteristics of the recording system.
M: relative magnification (amplitude/velocity).
(*a*) no filter, (*b*) high cut : 2.

The electromagnetic oscillograph (102A, Sanei Company) was driven at the maximum paper speed, 1m/sec. Accurate 1000cps signal controlled by piezo-mechanical fork was used for precise measurement of time. In many cases, galvanometers of 500cps in the natural frequency were used, except for a few cases in which 2000cps galvanometers were tried. Generally in this experiment the rock condition was so bad that resonance-like oscillation of cracked rocks on the adit wall obstructed normal detection of high frequency seismic waves. For this reason high frequency waves above 200cps could not help being cut in order to detect *S* wave. Accordingly, high frequency galvanometers were not necessary. Resultant characteristics of the apparatus, from a geophone to a galvanometer, are demonstrated in Fig. 6. The records used for the following discussion on wave form characteristics of *S* wave were obtained in the condition of curve (b) in Fig. 6.

§ Generation of *S* wave

In previous works[7][8], the author revealed *S* wave can be generated by a small explosion. The condition of seismic works in a adit protects the recognition of *S* wave from the obstacle of surface wave. For one record, a single drill hole, 0.7—1m in length, 3.6cm in diameter, was used as the shot hole. The shot holes were drilled horizontally and perpendicular to the adit wall. They are illustrated in Fig. 7. Geophones were installed on the pick-up bases cemented in short drill holes on the adit wall. Three elements observation of the oscillation could be made by setting three geophones on the

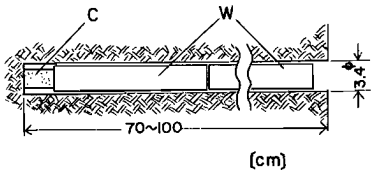

Fig. 7. Sketch of the shot hole.
C : charge.
W : water pouch.

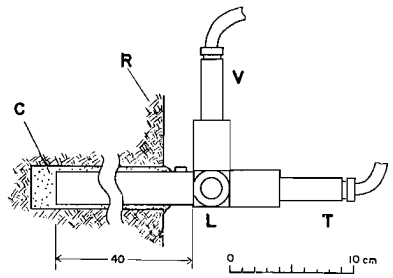

Fig. 8. Sketch of the geophone setting.
C : cement. R : rock. V, L and T : vertical, longitudinal and transverse component.

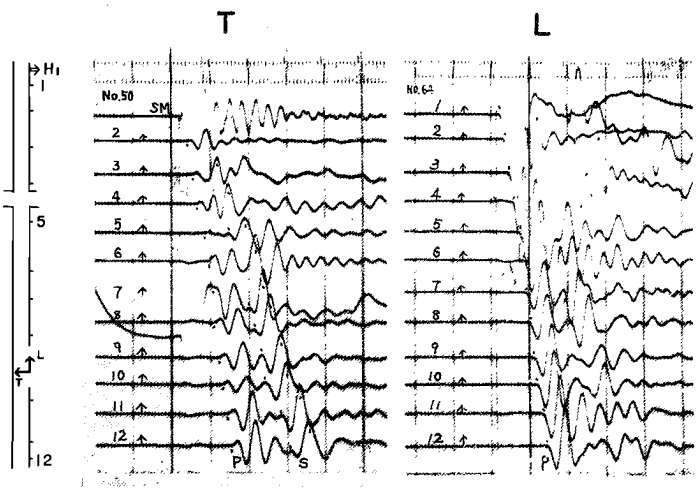

Fig. 9. Examples of the records. (explosion)

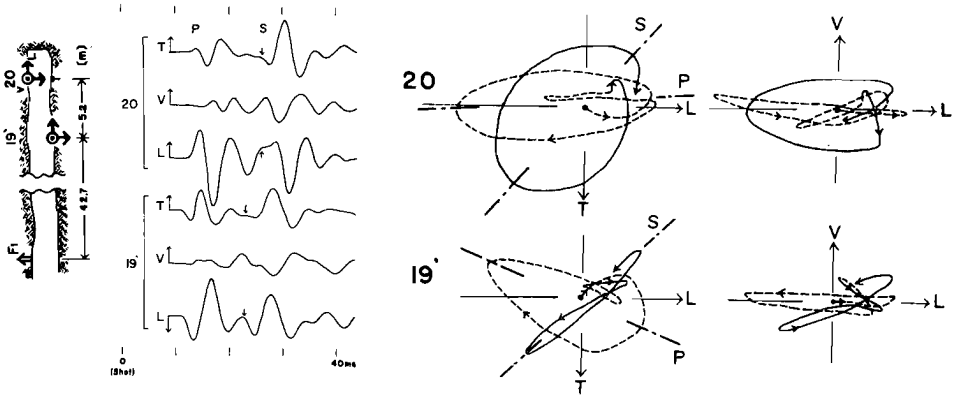

Fig. 10. Examples of the motional orbits. (explosion)
----P wave, ——S wave.

pick-up base. Details of geophone setting are demonstrated on Fig. 8.

Fig. 9 is an example of records obtained in the usual seismic line, in which case the geophones and shot point are located on the same straight adit. The motional orbits obtained from direct plotting of the records of the same kind are demonstrated in Fig. 10.

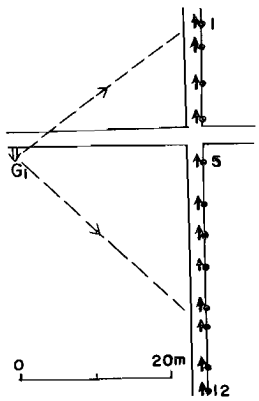

Fig. 11. Spread of geophones and a shot point for the experiment of *S* wave.

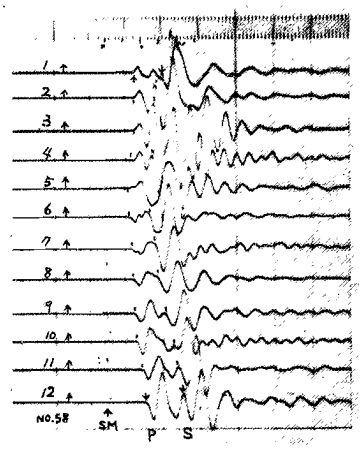

Fig. 12. The records obtained in the condition of Fig. 11. (explosion)

Although ideal orbits of wave phases can not be obtained, owing to the surface effects of adit wall, it is recognized that the principal direction of "*P* phase" oscillation is longitudinal and in many observational points the principal direction of "*S* phase" oscillation is nearly perpendicular to the former. Another evidence shows "*S* phase" is *S* wave. Fig. 11 illustrates the experimental procedure. Fig. 12 is the record obtained in this condition. "*S* phase" is clearly body wave because the propagation of this phase is not limited only in the near-surface of the adit.

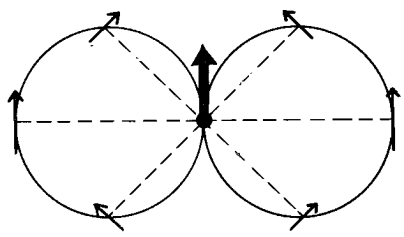

Fig. 13. Radiation pattern of *S* wave generated by the single force to which the effect of the small explosion illustrated in Fig. 7 is looked as identical, regarding the generation of *S* wave.

Directional characteristics of emission of *S* wave are an interesting problem in order to analize the mechanism of generation of this wave. The complete radiation pattern could not be obtained, because the field conditions were not adequate for this experiment. However, it is apparent that this wave has the polarization characteristics shown in Fig. 13, by synthesizing the separate experiments whose examples are shown in Fig. 14. Initial motions of *S* wave demonstrated in Fig. 14 mean only qualitative tendency of these directions, because *T* and *L* records were separately obtained.

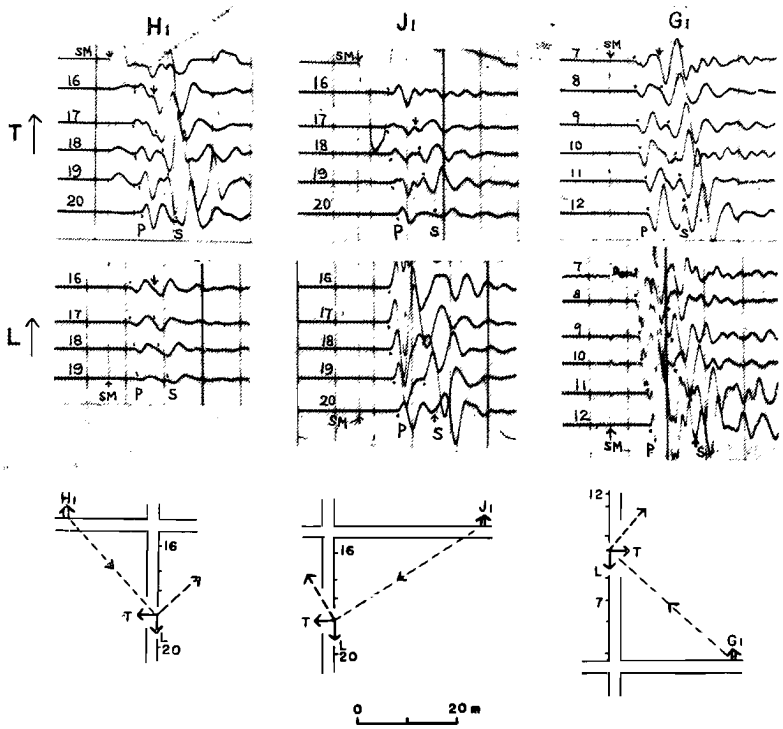

Fig. 14. Examples of records showing initial motions of S wave radiated from the small explosion.
Characteristics : G_1 – L ; (a) of Fig. 6, others ; (b).
←– – initial motion of S wave.

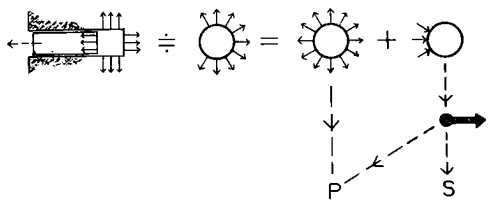

Fig. 15. Illustration of the mechanism of wave generation by a small explosion. A small explosion in a hole can be approximately treated as combination of an equi-expansive source and a single force.

This means the origin can be regarded as the single force[10], as far as it concerns the generation of S wave. This circumstance is illustrated in Fig. 15. Namely, the weak explosion (dynamite, 5–30g, in this experiment) in a hole can be approximately treated as combination of an equi-expansive source and a single force. By the latter S wave can be generated. In this case, the effect of the explosion will be equivalent to the effect of a hammer blow on a rock wall. Experiments showed that the records obtained by the hammer blow are nearly the same as those by the explosion. Examples of the records demonstrated in Fig. 16 show that the reverse of polarization occurs by reversing the direction of the hammer blow.

In the present experiment, S wave could be easily generated by the explosion in sound rocks. In cracked and weathered rocks, S wave was not domina-

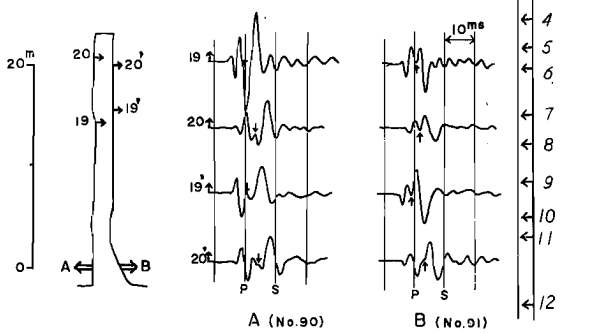

Fig. 16. Records obtained by the hammer blow. Phase of S wave is reversed by reverse of the blow direction.

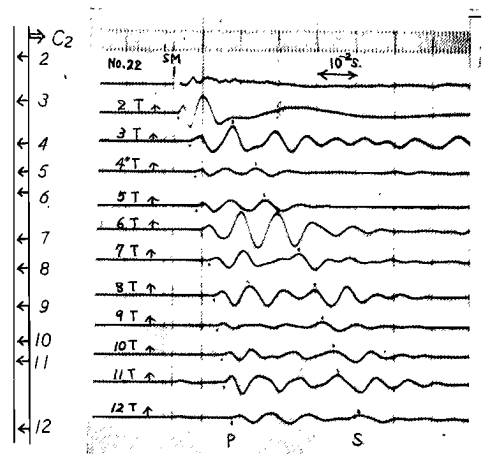

Fig. 17. An example of the records obtained in the weathered rock. (spread : $C_2 - E_1$ line)

ted by this method. This is due to the fact that the propagation of the waves was effected by the inhomogeneous states of the media. In this condition, even P wave was strongly disturbed as to its travel time and wave form. Noise-like oscillations, which appeared to be generated by the propagation along irregular wave paths and conversion of waves in inhomogeneous media, obstructed the clear recognition of S wave. Those examples are shown in Fig. 17.

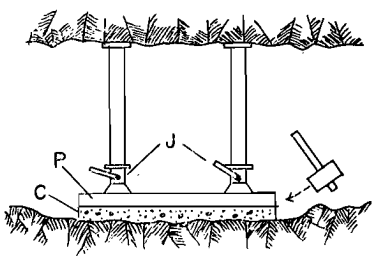

Fig. 18. Illustration of one of the methods tested for the generation of S wave.
P : wooden plate, 5×36×200cm.
J : jack.
C : concrete floor (10cm thick).

If the wave source purely originates only S wave, the circumstance will be much improved. For this purpose another method was tried. Fig. 18 illustrates this. A wooden plate is pressed with two jacks on a concrete base which is made in order to level a rock surface. This is struck with a hammer in the direction parallel to the plate surface. Even by this method, generation of P wave can not be avoided, but its proportion is much decreased, in comparison with that by the explosion method. In sound rocks, the wave trains of the transverse component obtained by this method practically begin with S wave. Such circumstances as this are demonstrated in Fig. 19.

In cracked and weathered rocks, the records are improved by this method only somewhat (Fig. 20).

Velocity of S wave was measured principally by the explosion method and partly by the plate-blow method. In many cases, velocity of P wave is also easily determined from the same records as ones for S wave. The measurements were carried out on the rock of every condition in the exploration adit.

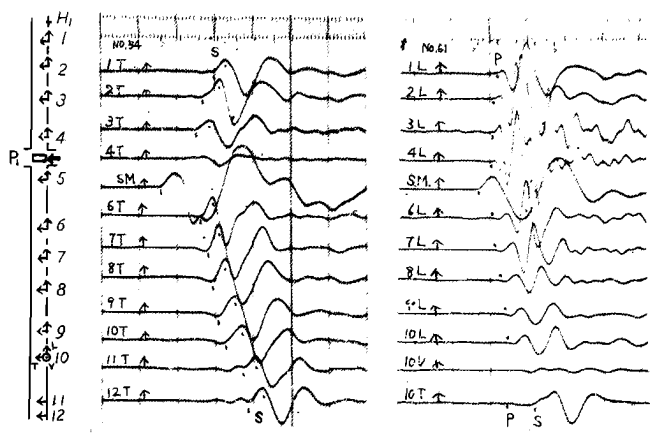

Fig. 19. Examples of the records obtained in sound rock by the method illustrated on Fig. 18. (source ; P_1 , geophone spread , H_1-J_1 line)

§ Determination of wave velocities

Method of analysis

(1) A troublesome problem in the determination of wave velocities is on the effect of the surface layer surrounding the adit. The layer of this kind is made secondarily by the effect of the adit excavation. This layer is cracked and in some cases weathered. So its wave velocities are lower than those of undisturbed rock surrounding it. For the determination of the velocities in undisturbed rock, the refraction method is useful. If the

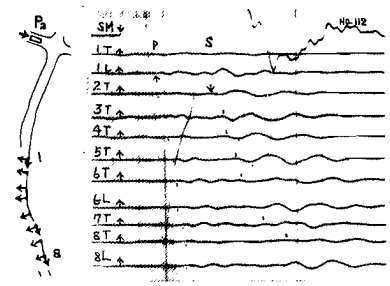

Fig. 20. An example of the record obtained in weathered rock by the method illustrated on Fig. 18.
(source , P_2, geophone spread ; E_1-F_1 line)

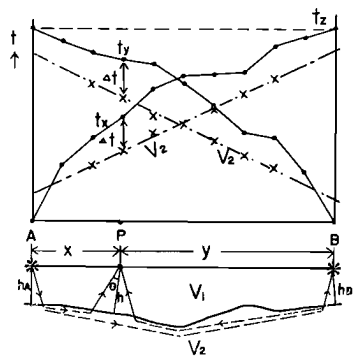

Fig. 21. Illustration of the "Hagiwara's method".
$\Delta t=(t_x+t_y-t_z)/2$, $h=v_1\Delta t/\cos\theta$.

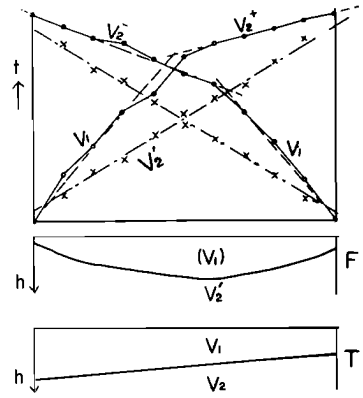

Fig. 22. False application of the "Hagiwara's method".
F : false, $V_1<V_2'<V_2$. T : true, V_2 ; based on V_2^+, V_2^- and V_1.

effects of the surface disturbed layer are not completely eliminated from the observed travel times, errors are more or less conducted into the analized velocities. The "Hagiwara's method"[9] is very useful for this analysis. This is the well-known method to eliminate the effect of the surface low velocity layer and to determine its thickness and the velocity of the underlying high velocity layer. The outline of this method is illustrated in Fig. 21. For the application of this method, the seismic line should be long enough that refraction ranges of the waves originated by the two end shots widely overlap.

In the short seismic line, identification on the direct and the refraction wave ranges is often so difficult that the results of analysis tend to contain error, owing to the incomplete separation of the ranges. This circumstance is illustrated in Fig. 22. On the determination of the velocities, the author was careful about this fact. When the "Hagiwara's method" cannot be applied, the ordinary analysis in case of two layer based on the assumption of monocline dip is adopted.

The analysis was done by the two method mentioned above. It was the author's principle to adopt the same method in the analysis for both P and S waves on the same seismic line. This is based on the assumption that there are not considerable differences between the structures for both P and S waves. In this paper, the most important quanta which can be experimentally obtained are the ratios of P and S wave velocities. Even if the adopted analitical method had not been adequate and therefore the absolute velocities determined by it had been somewhat erroneous, it should have been avoided that the determined α contained considerable errors based on different tendencies of analitical results. In this experiment, the travel time curve was often so complex owing to inhomogeneous properties of rocks, that this was necessary for useful analysis.

(2) In a curved adit, geophones and shot points can not be located on a straight line, that is, the seismic line is curved. For the analysis in this case, the "Hagiwara's method" was modified as follows. In Fig. 23, the curve APB is a seismic line. A and B are shot points. P is one of geo-

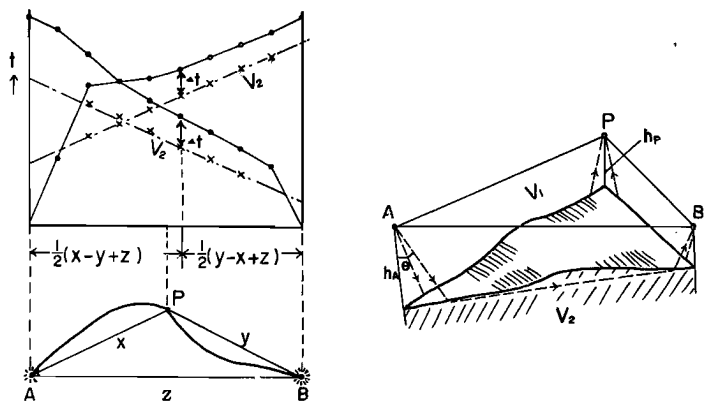

Fig. 23. Analysis on curved seismic line.

phones. We shall assume that projection of an individual wave path to the plane containing the seismic line (usually, horizontal plane) is practically a straight line. It means that the direction of layering effective to travel time of the waves is normal to the plane containing the seismic line (horizontal plane) as in the case of the ordinary seismic prospecting on the ground surface. The second meaning of this assumption is that the boundaries of different media are nearly normal to wave path and therefore the variation of the rock velocities can not be exactly evaluated in the region near a considerably curved seismic line. If the thickness of the surface layer is assumed to vary gently, as in case of the ordinal "Hagiwara's method",

$$\Delta t \equiv \frac{t_x + t_y - t_z}{2} = \frac{h_p \cos\theta}{V_1} + \frac{x+y-z}{2V_2} \qquad (7)$$

$$t_x - \Delta t = \frac{x-y+z}{2V_2} + \frac{h_A \cos\theta}{V_1} \qquad (8)$$

where t_x, t_y and t_z are the travel time of refraction wave in x, y and z, respectively. h_P and h_A are the thicknesses of the surface layer of positions P

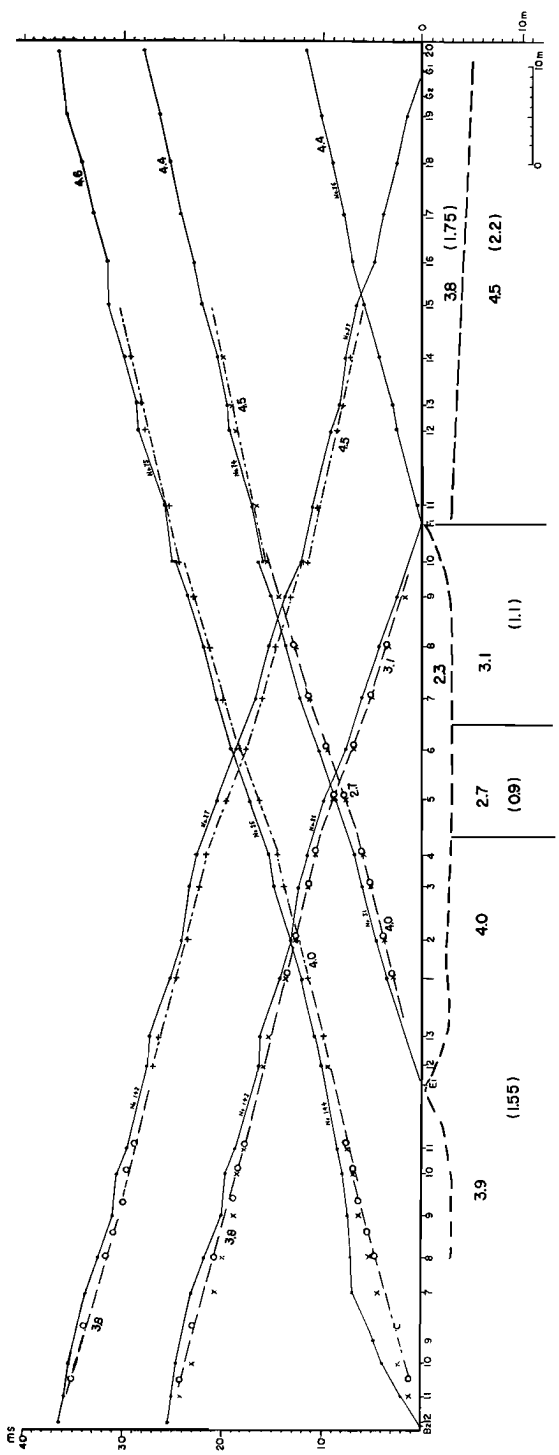

Fig. 24. (a). Travel time curve for P wave (spread : $B_2-E_1-F_1-G_1$ line) and the structures corresponding to P and S wave.
• initial kick, × +— — — $t_x-\Delta t$, ○— — — $t_x-\Delta t$ vs. $(x-y+z)/2$. Examples : $4.5=V_p$, $(2.2)=V_s$ (km/sec)

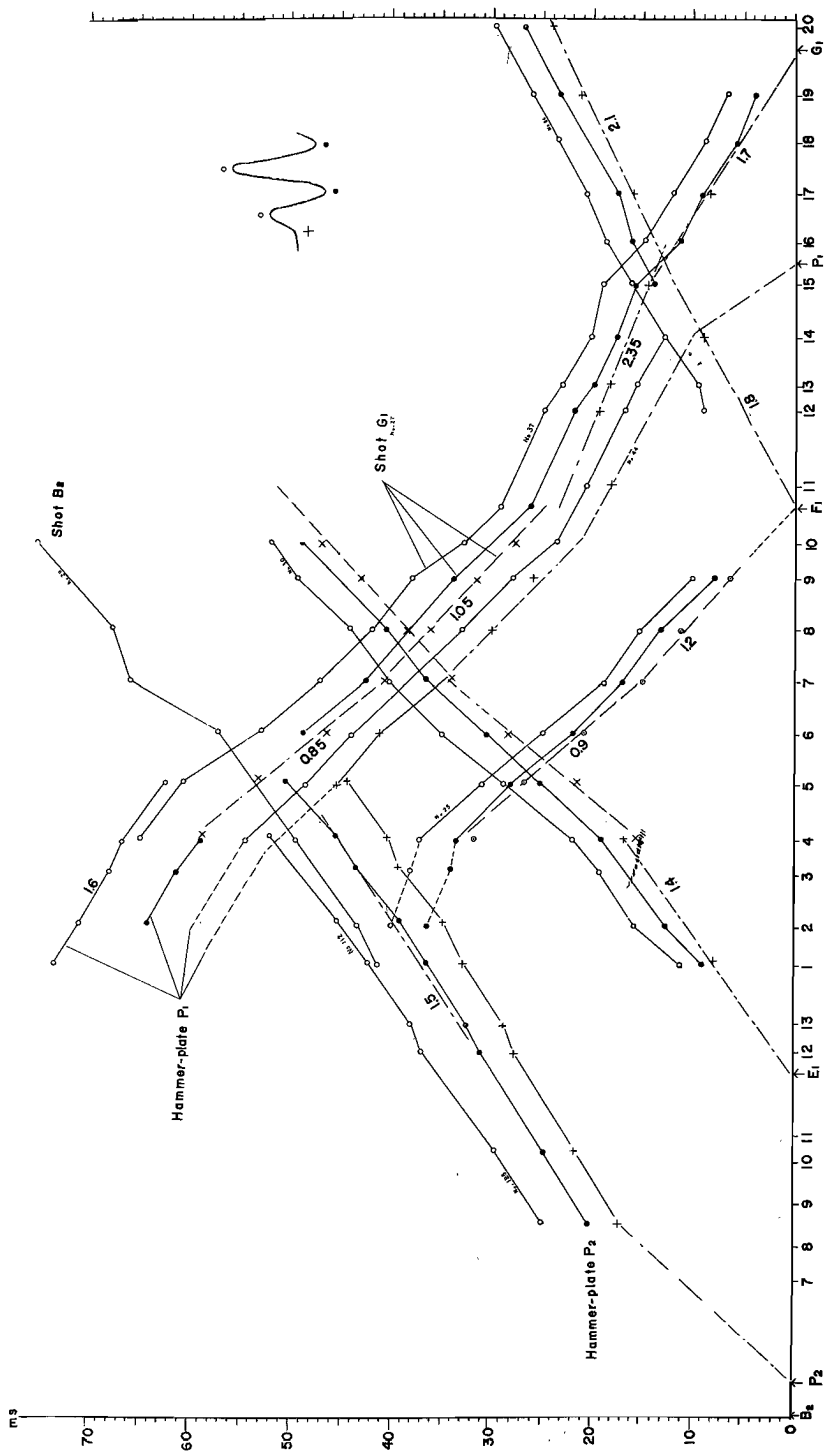

Fig. 24. (b). Travel time curve for S wave (spread : $B_2-E_1-F_1-G_1$ line).
$\times$ — — — $t_x-\Delta t$ vs. $(x-y+z)/2$.

and A. If $(x-y+z)/2$ is taken instead of x in Fig. 21, inverse gradient of the curve, $t_x-\Delta t$, gives the velocity of the underlying (or surrounding) layer, V_2. However, the thickness of the surface layer can not be directly given by Δt, as in case of Fig. 21. For the determination of the velocity (V_2), V_2 is not necessary to be constant. By the modification of Eq. (8), it is easily assured that its velocity variation can be similarly evaluated by the gradient variation.

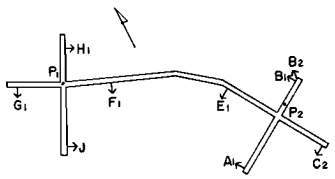

Fig. 24. (c). Main shot points.

Travel time curve

The travel time curves are shown in Figs. 24-27, whose respective places are found in Fig. 28 and Fig. 24 (c). In Fig. 24, the distance-coordinate is taken as the projection to the moderate standard line.

On the analysis of curved seismic line of this figure, the method (2) is used. The modified travel time curve, referring to $(x-y+z)/2$ and $t_x-\Delta t$ is partly added on the figure.

The velocities determined by the travel time curves are shown on the respective places of the map, Fig. 28, and Table 1. They are the undisturved velocities free from surface effect of the adit. The surface layer is omitted on the map. For reference, the velocity zones are drawn on this, which were determined by many other measurements in the adits and bore holes, as well as ones mentioned above.

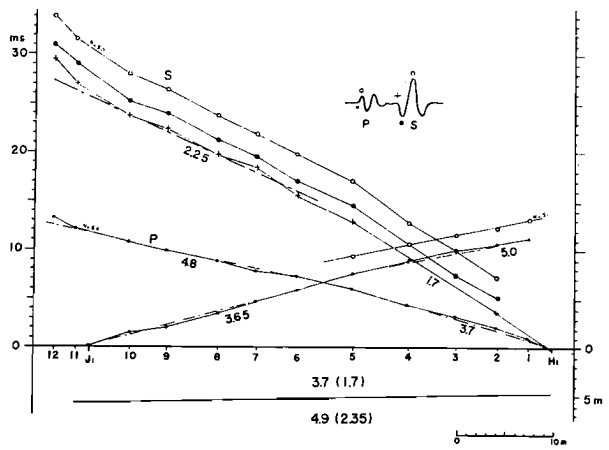

Fig. 25. Travel time curve for P and S wave (spread : J_1-H_1 line) and the structure obtained by the interpretation of them.

§ Discussion

Experimental formula

The most interesting problem for the author is the relation between α and V_p. This relation is demonstrated on Fig. 29, which shows clearly such a

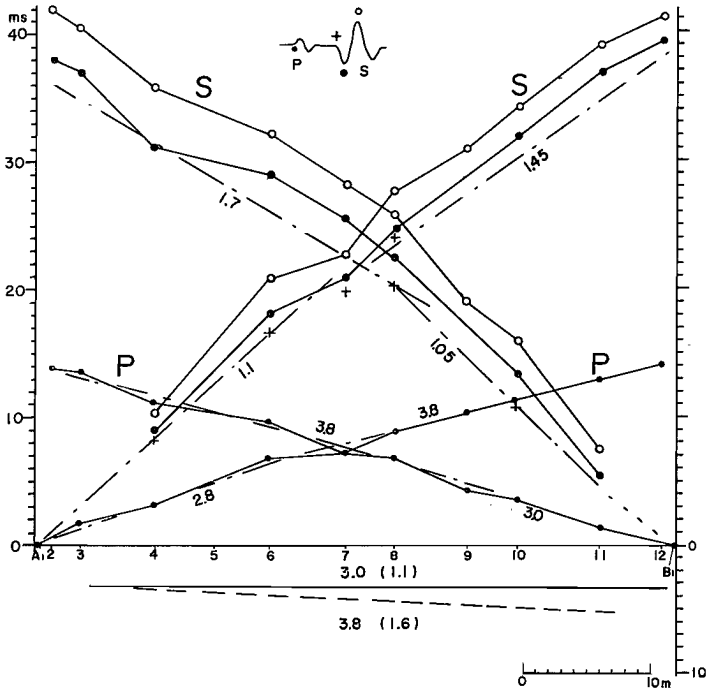

Fig. 26. Travel time curve for P and S wave (spread : A_1 – B_1 line) and the structures corresponding for them. (boundary ; — for P, --- for S)

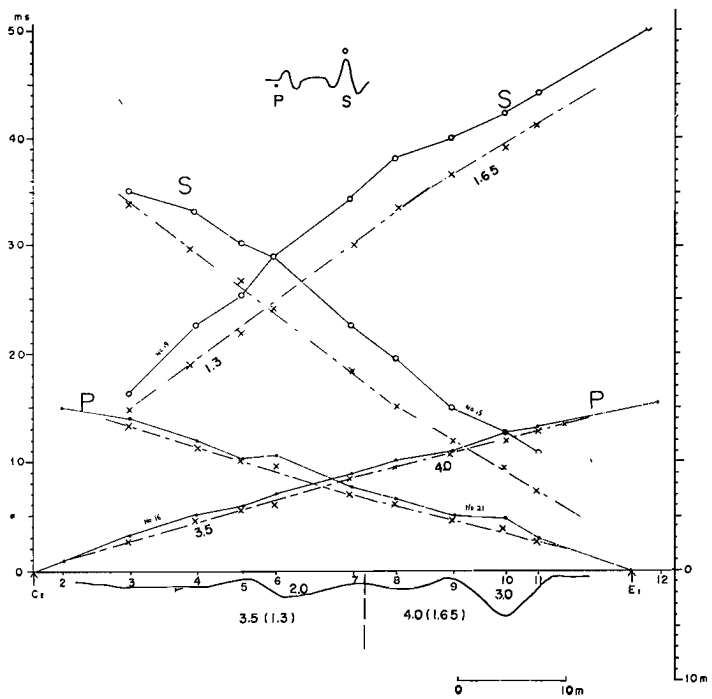

Fig. 27. Travel time curve for P and S wave (spread : C_2 – E_1 line) and the structures corresponding for them. (boundary ; — for P)

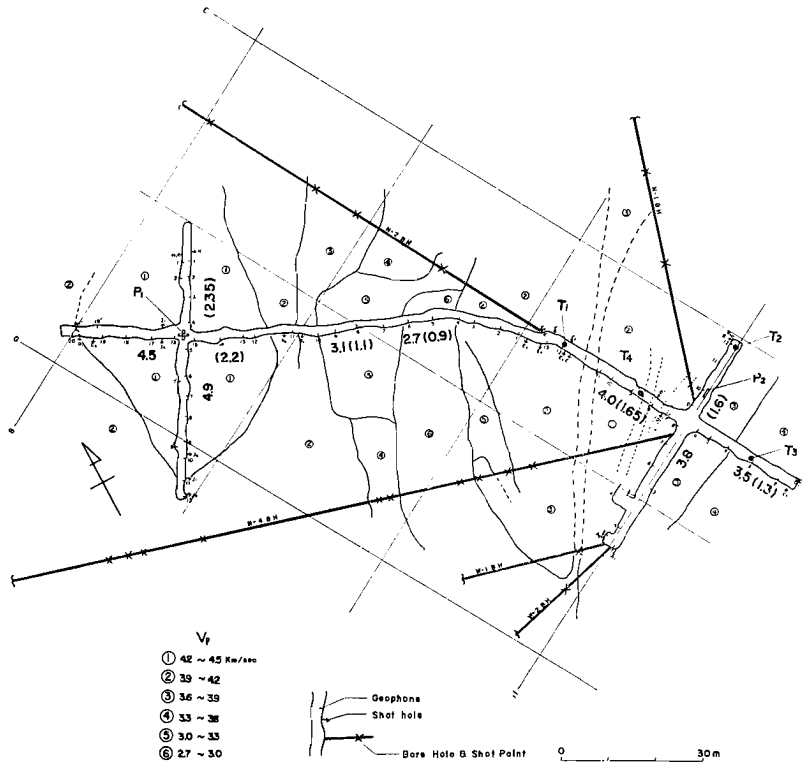

Fig. 28. The map showing positions of shots and geophones and the experimental results.

$T_1 \sim T_4$ · site of the jack test.

P_1, P_2 : the positions of the wave source illustrated in Fig. 18.

Wave velocities (km/s) 3.1 for P, (1.1) for S (examples).

TABLE 1.
Experimental results.

grade	V_P (km/s)	V_S (km/s)	$\alpha = V_P/V_S$	σ
C_H	4.9	2.35	2.08	0.350
C_H	4.5	2.2	2.05	0.344
C_M	4.0	1.65	2.42	0.405
C_M	3.8	1.6	2.38	0.392
C_M	3.5	1.3	2.70	0.421
$C_L \sim D$	3.1	1.1	2.82	0.428
D	2.7	0.9	3.00	0.438
(specimen)	5.36	3.20	1.68	0.225
	5.17	3.21	1.61	0.188
	5.43	3.45	1.57	0.160
	4.85	2.98	1.63	0.199

tendency as α increases with decrease of V_p. Possible errors are thought to be about 3% for the P wave velocity and 6% for the S wave. Accordingly, possible error of V_p/V_s is nearly 10%. The relation between α and V_p, $\alpha=\psi(V_p)$, shall be assumed to be a linear equation. Its formula is determined by the means of the least square as follows,

$$\alpha \equiv V_p/V_s \equiv \psi(V_p) = -0.49V_p + 4.34 \tag{9}$$

For reference, the data obtained in situ on granite of other places are also plotted on Fig. 29. The supersonic test was also carried out for a few rock specimens obtained from bore holes in this field. They are thought to give the values of the sound rock.

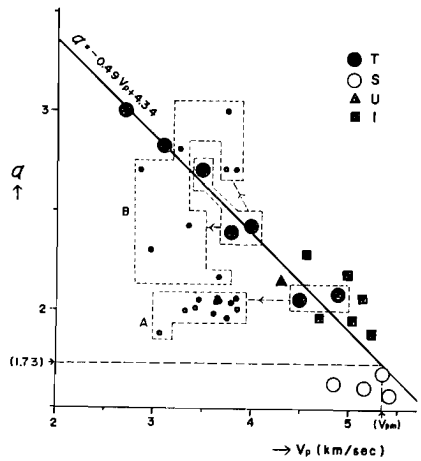

Fig. 29. Plotting of the experimental results.
Tsuruga . T; in situ (Experimental formula is determined for this.)
S; specimen (dry up in room temperature).
A, B; including the surface effect.
Ushimado : U, Ikoma : I ; in situ.

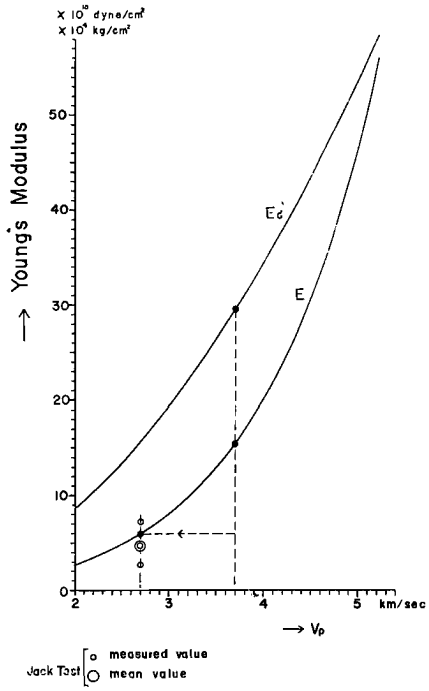

Fig. 30. Variation of Young's modulus in granite.
E : Young's modulus evaluated according to the experimental formula in Fig. 29.
E'_d : the "conventional Young's modulus" ($\sigma=0.25$).

Thus we have obtained the relation between V_p and α. By Eqs. (3), (4) and (6) true Poisson's ratio and dynamic Young's modulus can be easily calculated. The latter is shown in Fig. 30.

Comparison between the dynamic method and the static

The result mentioned above shall be compared with the values by the jack test of which position is shown in Fig. 28. Definition of the Young's modulus in this case is illustrated in Fig. 31. The value of Young's modulus by this

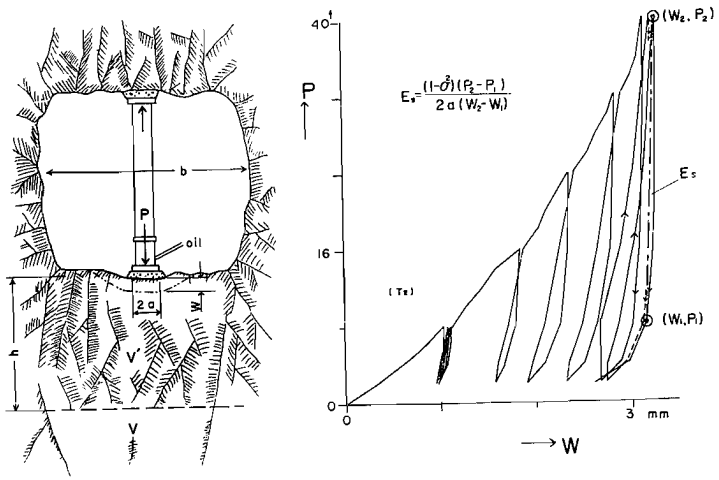

Fig. 31. Illustration of the jack test and the definition of static Young's modulus E_s.
W : displacement. $V'=kV$ $(k<1)$.
P . load. a . radius of load plate.

TABLE 2.
Results of the jack test.

No.	site	E [10^4kg/cm^2]	direction of pressure	note
1	T_1	4.84	horizontal	
2	T_2	7.31	vertical	
3	T_3	0.46	vertical	shear zone
4	T_4	2.7	vertical	

method is not practically affected by Poisson's ratio, because $\sigma^2 \ll 1$.

This test was carried out by a company. The results are shown on Table 2.

The sites of the jack test are inhomogeneous, and their rock conditions are not the same. The velocity of the surface layer should be adopted as ones corresponding to the jack test, because its thickness h(3–5 m) is much larger than the radius of the load plate, a(15 cm). Evaluation of Young's modulus by the jack test is based on the assumption that a circular plate load is applied to the surface of semi-infinite elastic medium. Normal stress in the depth d decreases to less than 1/50 of that in the surface, when $d/a>10$[13]. Accordingly, the effect of h to the evaluation of the Young's modulus can be practically neglected, if $h/a>10$. The exact velocity of the jack test site, point by point, can not be evaluated, and it is not necessary for the present step of the discussion. We adopt 2.7 km/s as the mean velocity of P wave in the surface layer whose measured velocity is 2.3–3.0 km/sec. Density of the rocks determined by the laboratory experiment shows the values very near to 2.7 g/cm^3. If we assume Eq. (9) can be also applied to the surface layer, Young's modulus is determined as 6.0×10^4 kg/cm^2, which is shown in

Fig. 30. Validity of this assumption was not completely assured in those sites, as mentioned later.

The value of the jack test No. 3 was obtained on the site particularily different from the mean condition through the whole those sites. Therefore, this value should be rejected at the evaluation of the mean value of the jack tests. In this case it is determined as 4.9×10^4 kg/cm^2. Two Young's moduluses coincide each other sufficiently as such kind of discussion. If we assume Poisson's ratio as 0.25 conventionally and disregard velocity lowering in the surface layer (V_p=3.7 km/sec. is adopted as the mean value), we obtain 29.5 $\times10^4$ kg/cm^2 as Young's modulus. Such Young's modulus shall be especially called as "conventional dynamic modulus" in this paper. This is about six times the value by the jack test. That coincides approximately with the results obtained by several authors.

According to this experiment, considerable discrepancy between the values by those two methods is not found. As shown in Fig. 30, Young's modulus is lowered to about a half of the conventional one, owing to adopt real Poisson's ratio. Considering the velocity lowering in the surface layer, Young's modulus moreover falls to about half. Total lowering is about one fourth or one fifth.

Generalization of the experimental result

(1) As the author does not have enough data on many kinds of rock, he can not give the direct evidence to assure that the explanation mentioned above can be generalized to the problem on the discrepancy of the static and the dynamic modulus in all kinds of rock. However, a suggestion on this problem is proposed by the following means.

It shall be assumed that the static Young's modulus in situ is equivalent to the dynamic Young's modulus modified by the effect of the variation of Poisson's ratio and that of velocity lowering in the surface layer. The modulus defined by the above interpretation, E_s', is expressed as follows.

$$\left.\begin{aligned} E_s' &= \rho k^2 V_p^2 F(\alpha_k) \\ \alpha_k &= \psi(kV_p) \end{aligned}\right\} \tag{10}$$

where k is the effective reduction ratio of P wave velocity in the surface layer, compared with one of the surrounding rock (V_p). The function ψ is assumed to be expressed by Eq. (9).

The "conventional dynamic Young's modulus" E_d' is defined as follows.

$$E_d' = \rho V_p^2 F(1.73) \tag{11}$$

V_p=1.73 corresponds to σ=0.25. k=0.75 is thought to be reasonable in common conditions as the first approximation, as known from the examples in Table 3, though the value of k is affected by state and kind of rocks.

The relation between E_s' and E_d' can be directly determined from Fig. 30. It is demonstrated in Fig. 32.

The relation between Young's modulus by the jack test (E_s) and one by the seismic method ("conventional modulus" E_d) was investigated by T. Onodera[2]. The curve (E_s) shown in Fig. 32 was given by him as the representative

TABLE 3.
Velocity reduction due to the surface effect.

rock	place	V_P [km/s]	V'_P [km/s]	k $(=V'_P/V_P)$	h [m]
granite	Tsuruga	4.5−4.9	3.0−3.8	0.72*	3−5
		3.5−4.0	2.3−3.0	0.70*	2−5
		3.5	2.6	0.74	
granite	Ikoma	4.7	3.9	0.83	2−4
		5.2−5.3	(5.2−5.3)	(1)	0
		3.4	1.3	0.38	1−2
slate	Shiroyama	4.2	1.7	0.40	1−3
		4.4	1.9	0.43	1−4

V_P : velocity (P) undisturbed by the surface effect.
V'_P: velocity (P) of the surface layer.
h : thickness of the surface layer.
* : ratio for the mean velocities.

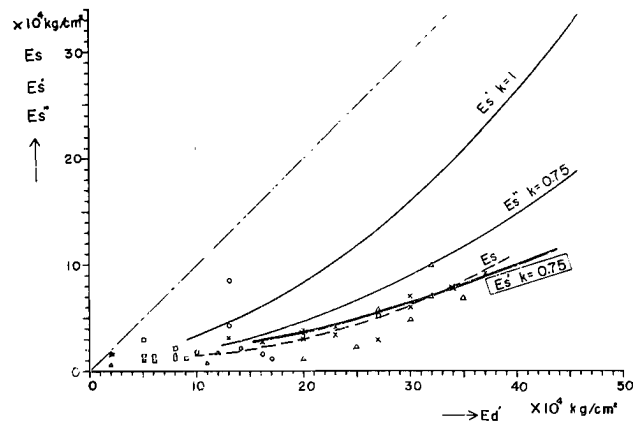

Fig. 32. Comparison of E'_s with E_s.
The curve E_s and plotted points (measured values of E_s) are cited from T. Onodera's paper.

tendency of the relation, although the points were fairly scattered. E'_s in case of $k=0.75$ well coincides with E_s. In Onodera's relation the kind and the state of rocks were not classified, but they were mixed.

The problem to be studied is whether the relation α vs. V_p in the surface layer is the same as in the undistured rock surrounding it. Its direct measurement was difficult in the usual refraction line because of the irregularity of rock condition in the surface layer and of its thinness. The velocities obtained in such a condition as shown in Fig. 11, give a suggestion for the above problem. The velocity defined by the ratio between straight distance of a shot point to a geophone and the travel time is strongly affected by the velocity of the surface layer, because the thickness of the surface layer, 3—5 m (effective value is twice this), is relatively large, compared with the

straight distance, 20—30 m. The velocity ratios in this case are plotted in Fig. 29 with particularily distinguished marks. Their connections to the values of the "undisturbed rocks" in the same places are shown in this figure. In Group *A*, high velocity range, the relation of α vs. V_p does not follow the general tendency of the "undisturbed rock". α in the surface layer remains approximately as it is in the original undisturbed rock. In Group *B*, low velocity range, the tendentious discrepancy can not be found between them, partly because of the wide scattering of points owing to the inhomogeneous condition that obstructs clear detection of the relation. The jack tests were carried out at this site.

Based on the preceding discussion, for reference, other possible Young's modulus of the surface layer is shown in Fig. 32. It is evaluated on the assumption as follows. α of the "undisturbed rock" is also conserved in one of the surface layer, and the coefficient of the velocity lowering in it, k, is 0.75. Hence,

$$E_s'' = k^2 V_p^2 F(\alpha) \tag{12}$$

where $\alpha = \psi(V_p)$. $\psi(V_p)$ is assumed to be expressed by Eq. (9).

(2) Many experiments have confirmed that α in sound rocks have the values very near 1.73 ($\sigma = 0.25$). Accordingly, if the experimental result of granite can be generalized, α should be expressed by V_p/V_{pm} instead of V_p, where V_{pm} is the maximum velocity of P wave of the relevant rock (the velocity of the rock free from weathering effects). In Fig. 29 we take the value of V_p which corresponds to $\alpha = 1.73$, as V_{pm}. It is 5.34 km/sec. Considering the result of the supersonic measurement on the sound rock specimens in this field, this is a reasonable value. Hence, Eq. (9) is modified as follows.

$$\alpha = -2.61\beta + 4.34 \tag{13}$$

where $\beta = V_p/V_{pm}$. By this relation $F(\alpha)$ can be expressed by β.

$$F(\alpha) = \phi(\beta) \tag{14}$$

On the other hand, H. Masuda investigated the relation between the "conventional" dynamic Young's modulus (E'_d) by the seismic prospecting and the Young's modulus (E_R). E_R is the value which has been adopted by many projectors for concrete dams according to their judgement. He proposed the following formula as the first approximation for this relation.

$$E_R = \frac{1}{2}\frac{V_p}{V_{pm}} E'_d = \frac{1}{2}\beta f(\sigma)\rho V_p^2 \tag{15}$$

where $\sigma = 0.25$. The Masuda's coefficient $\beta/2$ was proposed for correction of the "conventional" dynamic Young's modulus so that it might be applied for engineering projects. In order to compare E_R with the real dynamic Young's modulus E in Eq. (4), it suffices to compare $\beta f(0.25)/2$ with $\phi(\beta)$. In Fig. 33 they are mutually compared.

There is not a considerable discrepancy between them in the region of $\beta <$ 0.8, which is the most common case.

From the preceding discussion it is suggested that there is not a considera-

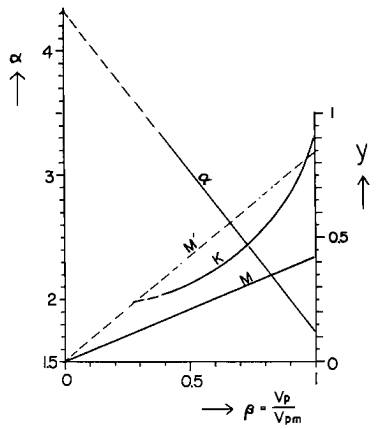

Fig. 33. Comparison between $\phi(\beta)$ and "Masuda's formula".
K . $y=\phi(\beta)$.
M : $y=0.417\beta$ ("Masuda's formula")
M' : $y=2\times0.417\beta$.

ble discrepancy between the "true" dyamic Young's modulus in situ (E) and the one used for engineering design (E_R). The Masuda's coefficient will be replaced by the ordinary effect of Poisson's ratio as the first approximation.

§ Conclusion

In situ ratio of P and S wave velocities (α) and Poisson's ratio (σ) were measured for various weathering states in granite. α approximately increases linearly with decrease of P wave velocity (V_P). When the ratio of V_P to its maximum velocity (V_{Pm}) decreases to 1/2, α increases to about 3 ($\sigma=0.44$).

Rocks in this field are thought to be saturated by water. For the different conditions and kinds of rocks, different results may be obtained. Further discussions of this is our future problem to be studied. If the present experiment can be extended to common rock, the discrepancy between the "conventional" dynamic Young's modulus and the static one in situ can be explained approximately by the effect caused by neglect of variation of Poisson's ratio in situ. Partly, that should also owe to the neglect (or incomplete correction) of the velocity lowering in the surface layer.

It is thought that expression of elasticity of rock by Poisson's ratio is not practically adequate, because it approaches rapidly to the limit value 0.5 with a little increase of α. For example, $\alpha=3$ is not an uncommon value, considering that $\alpha=5$ is very common in sand and gravel[11)12)]. But $\sigma=0.44$ which corresponds to $\alpha=3$, tends to give the impression that the state expressed by it is very liquid and not common. In consideration of the effect of Poisson's ratio, several investigators discussed only on the range very near to $\sigma=0.25$. The author believes that α is more adequate than σ for practical evaluation of the rock state.

Strictly speaking, this paper discusses only the comparison between the dynamic elastic properties in the particular range of stress and stress rate and the static Young's modulus defined according to particular engineering consideration. It is obvious that rock properties in situ are not completely elastic, but rather viscoelastic and plastic or more complex. According to the author's belief, only what cannot be explained by complete elastic treatment should be discussed in connection with inelastic properties of rock.

Acknowledgement

The author wishes to thank Prof. K. Sassa, who stressed the necessity of the study on the true value of Poisson's ratio and its applications to many practical fields before popular attention began to be paid to those problems.

The author also appreciates Prof. S. Yoshikawa's support for practice of the field experiment. Mr. N. Gotō, Mr. A. Kitazumi, Mr. T. Ikawa and Mr. I. Nishizaki cooperated with the author in the field experiment. The author thanks them also.

Appendix

Tanaka's Classification on the Feature of Rock[14]

Name	Characteristics of the rock
A	The rock is very fresh, and the rock-forming minerals and grains are neither weathered nor deteriorated. The cracks and joints closely adhere to one another. No trace of weathering is found along their surface.
B	The rock is solid. Neither crack (of even 1 mm.) nor joint is opened. They closely stick. But the rock forming minerals and grains are partially attacked by slight weathering and deterioration.
C_H	The rock forming minerals and grains excluding quartz are slightly softened by the weathering action. In general, the rock is stained by the limonite, etc.
C_M	The rock forming minerals and grains excluding quartz are a little softened by the weathering action. If it is struck, it peels off along the joints or cracks. On the broken off surface, the thin layer of red and, or brown clay materials exist.
C_L	The rock forming minerals and grains excluding quartz are fairly softened by the weathering action. If it is slightly struck, it peels off along the joints or cracks and breaks into little pieces. Rock is much jointed and cracked. Among joints or cracks, the thin layer of red and, or brown clay materials exist.
D	(1) Affected by the weathering action, the rock-forming minerals and grains are deteriorated, turned yellow-brown or brown, and the rock is remarkably softened. (the rock which looks like the weathered rock to anybody) (2) On the rock-bed, there is found a developement of opened large cracks or joints. The rock-bed is subsequently divided into several lumps. Though each rock lump is sound, the opened cracks or joints can inhale the smoke, or the fire of handlamp. (3) In addition, the fine roots of trees penetrate into the joint or crack surface of the rock-bed.

(After Tanaka's paper)

References

1) Masuda, H. : Geophysical Exploration of the Dam Foundation, Butsuritanko (Geophysical Exploration), 13, 1960, pp. 25–35 (in Japanese).
2) Onodera, T. : General Note on the Geophysical Prospecting in the Construction Ministry, Butsuritanko, 13, 1960, pp. 65–72 (in Japanese).
3) Jad, W. R. : Rock Stress, Rock Mechanics, and Research, State of the Stress in the

Earth Crust (International Conference held at Santa Monica, California, June, 1963), pp. 5–54, Elsevier, New York.
4) Wantland, D. : Geophysical Measurement of Rock Properties in Situ, do., pp. 409–450.
5) Love, A. E. H. : A Treatise on the Mathematical Theory of Elasticity, p. 103, p. 297, Dover, New York.
6) Kusakabe, S. : A Keinetic Measurement of the Modulus of Elasticity for 158 Specimens of Rocks, and a Note on the Relation between the Keinetic and Static Moduli, Pub. E. I. C. No. 22, 1906, B, pp. 27–49.
7) Kitsunezaki, C. : Study of High Frequency Seismic Prospecting (1), Butsuritanko, 13, 1960, pp. 102–107, pp. 137–146 (in Japanese).
8) Kitsunezaki, C. · High Frequency Seismic Prospecting, Geophys. Papers Dedicated to Professor Kenzo Sassa, pp. 179–185.
9) Hagiwara, T. · Butsuritanko, Asakura-shoten, Tokyo, 1951, p. 23.
10) White, J. E. . Seismic Waves, McGraw-Hill, New York, 1965, p. 214.
11) Yoshikawa, S., Shima, M. and Gotō, N. : On the Seismic Prospecting at the Area Damaged by Niigata Earthquake, Disaster Prevention Res. Inst. Annuals, No. 8, 1965, pp. 19–34.
12) White, J. E. and Sengbush, R. L. : Velocity Measurements in Near-surface Formations, Geophysics, Vol. 18, 1953, pp. 54–69.
13) Terzaghi, K. : Theoretical Soil Mechanics, John Wiley and Sons Inc., New York, p. 489.
14) Tanaka, H. : Geology of the Dam and the Treatment of its Foundation, Technical Report (Central Res. Inst. of Electric Power Industry) C-6203, 1963, p. 25.